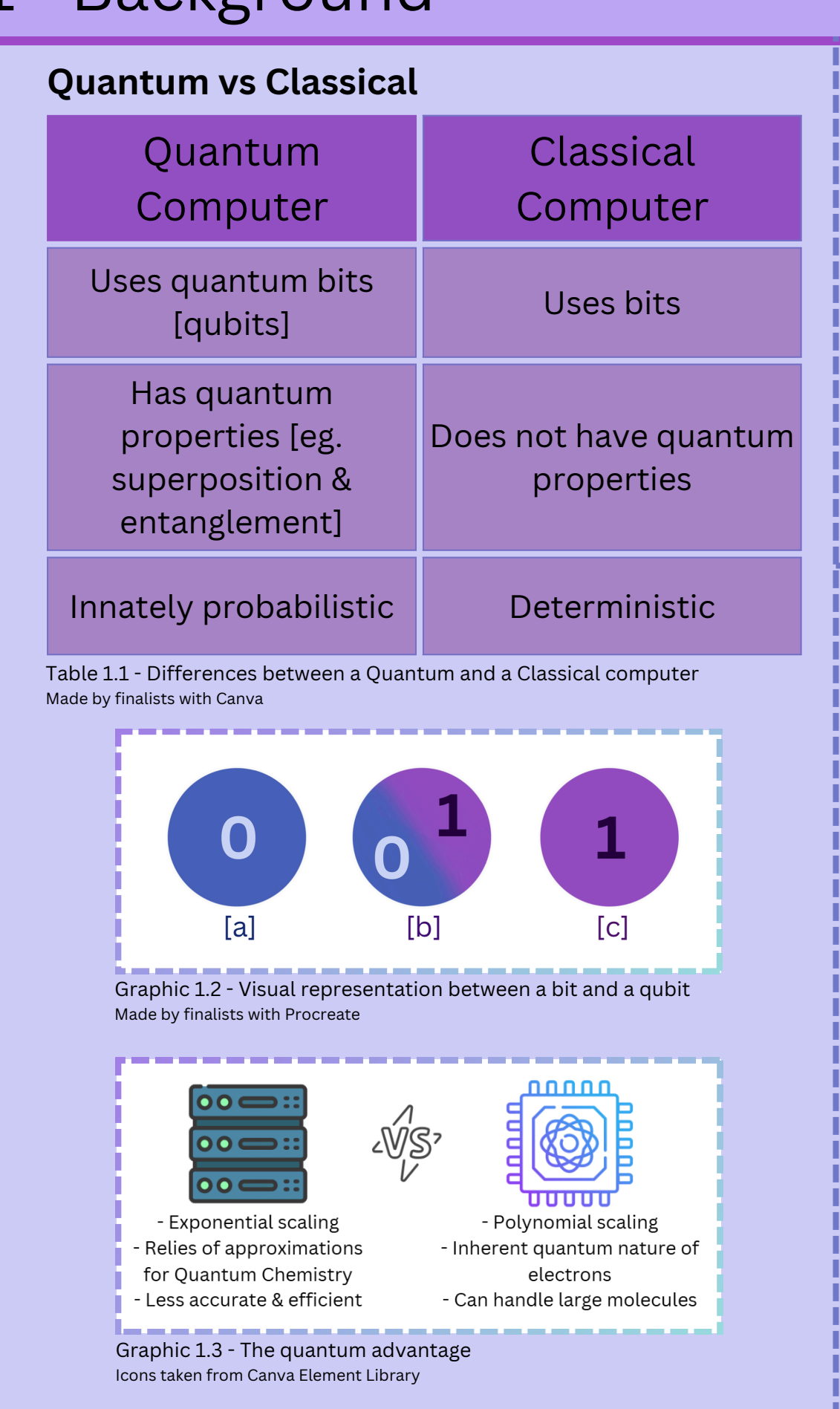
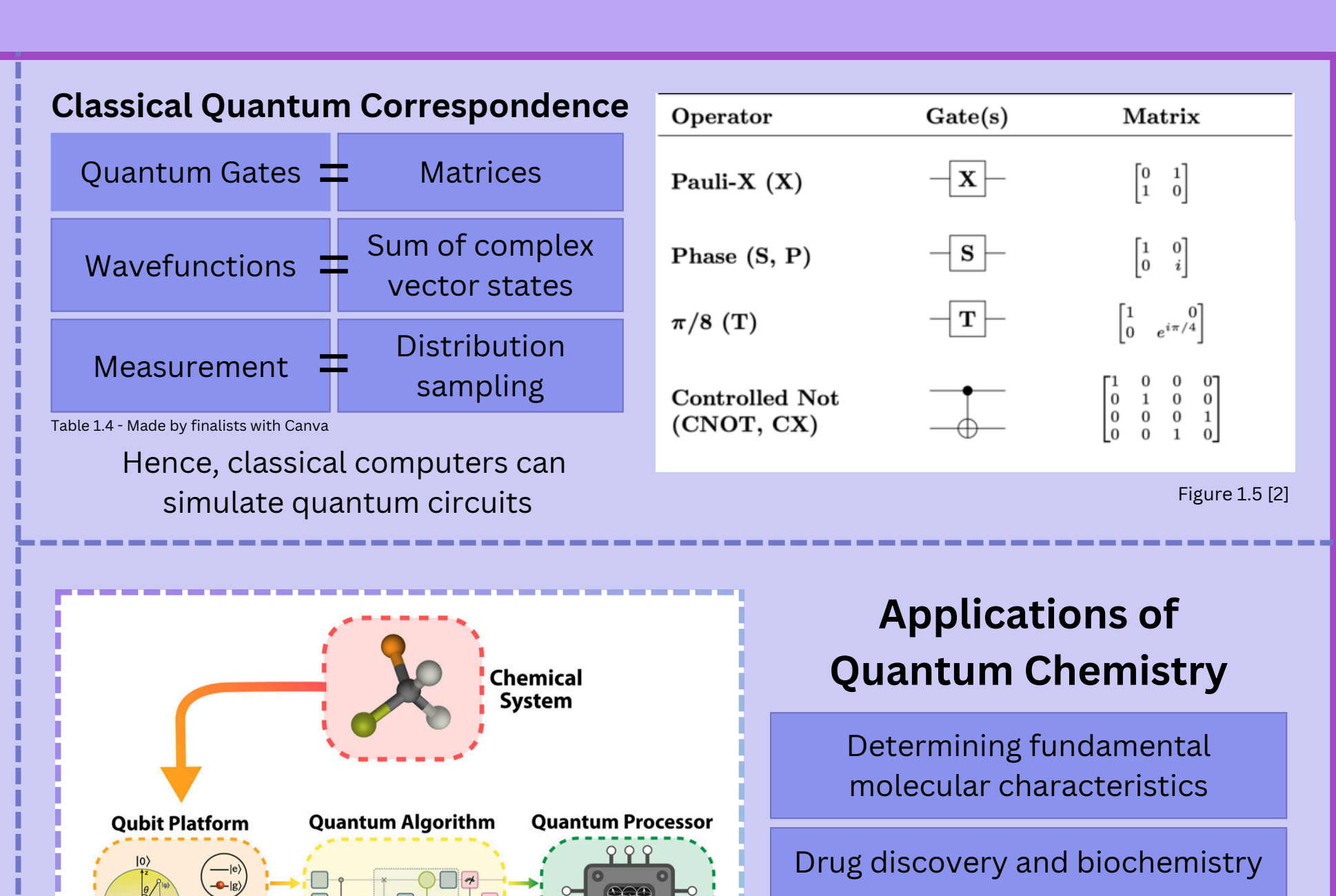
Modelling the Hydrogen Molecule (H2) with Quantum Circuits

Cai Shuce Liu Shuyu







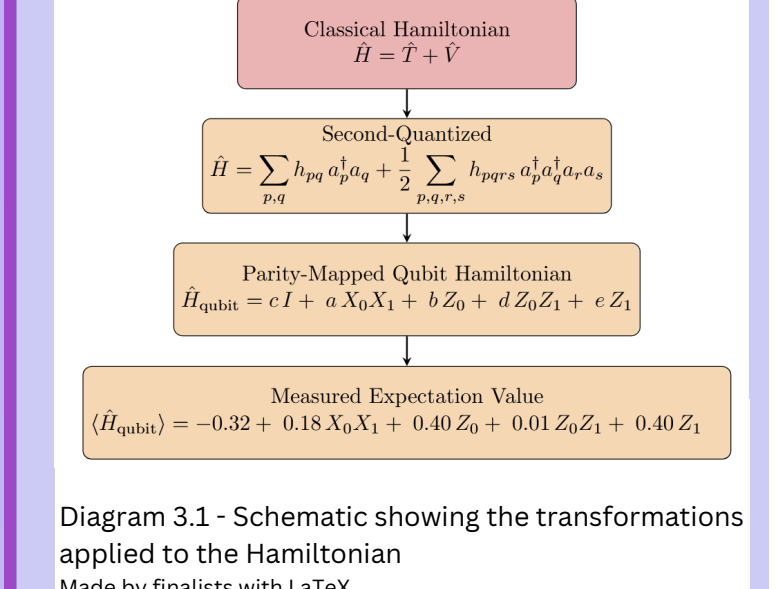
Innovations in material science (nanotech, superconductors, etc) **Quantum Cloud Computing** Integrations in engineering processes and solutions Analyse catalytic and reaction mechanisms Graphic 1.6 - Schematic showing how Quantum Computational Chemistry is Table 1.7 - Made by finalists with Canva carried out on Ouantum Computers [1]

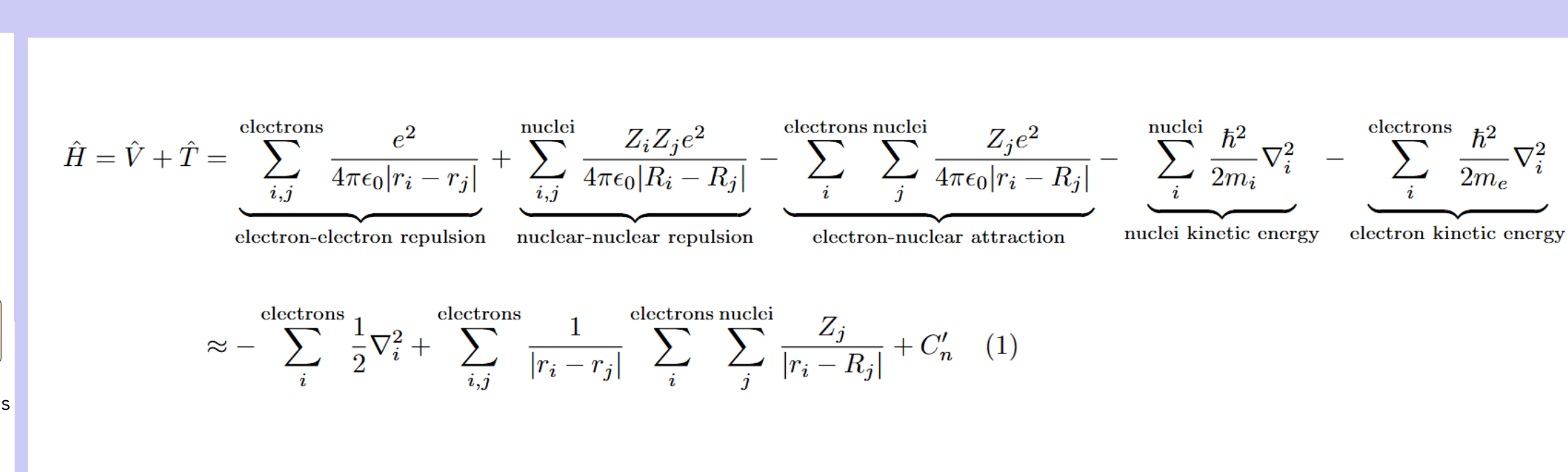
2 - Objective

- Assess the effectiveness and accuracy of the Variational Quantum Eigensolver [VQE] in computing molecular ground state energies and molecular geometry
- Quantitatively characterise the **effects of noise**, in particular thermal relaxation noise, on simulation outcomes
- Develop a well documemted, streamlined framework for future researchers that leverages the VQE approach

3 - Hamiltonian Representation

The Hamiltonian is the sum of potential and kinetic energy of particles in the system. The Born-Oppenheimer **Approximation** is used to assume the nucleus as stationary and hence the nuclear repulsion energy as a constant C'n. Atomic units [$\hbar = m_e = e = 4\pi\epsilon_0 = 1$] are used to simplify the expression further.





4 - Methodology [VQE - Varitional Quantum Eigensolver]

1. Second Quantisation

Accounts for fermionic properties [Pauli Exclusion Principle]

3. Ansatz Preparation [UCC - Unitary Coupled Cluster]

UCC approximates a molecule's wavefunction by applying a unitary

exponential operator to a reference state, typically the Hartree Fock [HF]

 $|\Psi_{\rm UCC}\rangle = e^{T-T^{\dagger}}|\Phi_{\rm HF}\rangle$ (9)

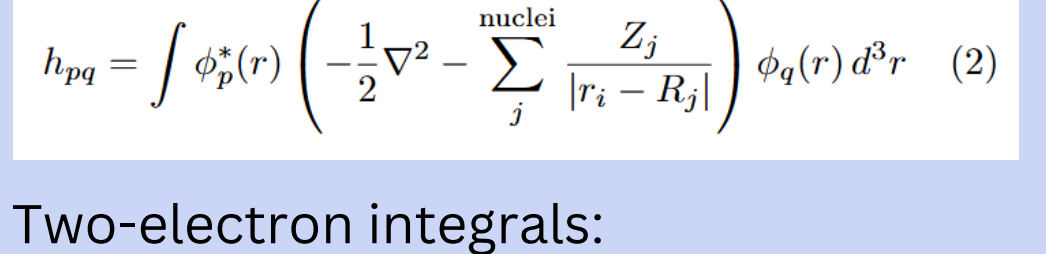
electron density in different orbitals.

 $\hat{T} = \hat{T}_1 + \hat{T}_2 = \sum_{i,a} \theta_i^a a_a^{\dagger} a_i + \frac{1}{4} \sum_{i,j,a,b} \theta_{ij}^{ab} a_a^{\dagger} a_b^{\dagger} a_j a_i$ (8)

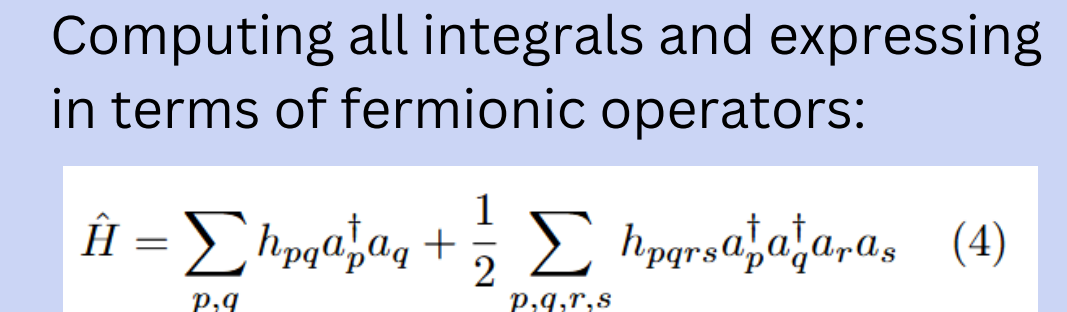
state, which is an initial approximation of the molecule's ground state.

- Easier to solve for **pairwise** electron interactions.
- Transforms continuous problem to discrete, matrix-like form
- Formulated with a **finite set of orbitals** [i.e. STO-3G], each being a solution to the Schrödinger equation

One-electron integrals:



 $h_{pqrs} = \int \int \frac{\phi_p^*(r_1)\phi_q^*(r_2)\phi_r(r_2)\phi_s(r_1)}{|r_1 - r_2|} d^3r_1 d^3r_2 \quad (3)$



H₂ HF state and

excitation parameters

Spin-Orbital Mapping $|\Psi_{HF}\rangle = |1100\rangle$:

(virtual spin-orbital for α)

 $|0\rangle_3 \to 2\beta$ (virtual spin-orbital for β)

 $|1\rangle_1 \to 1\beta$ (occupied spin-orbital for β)

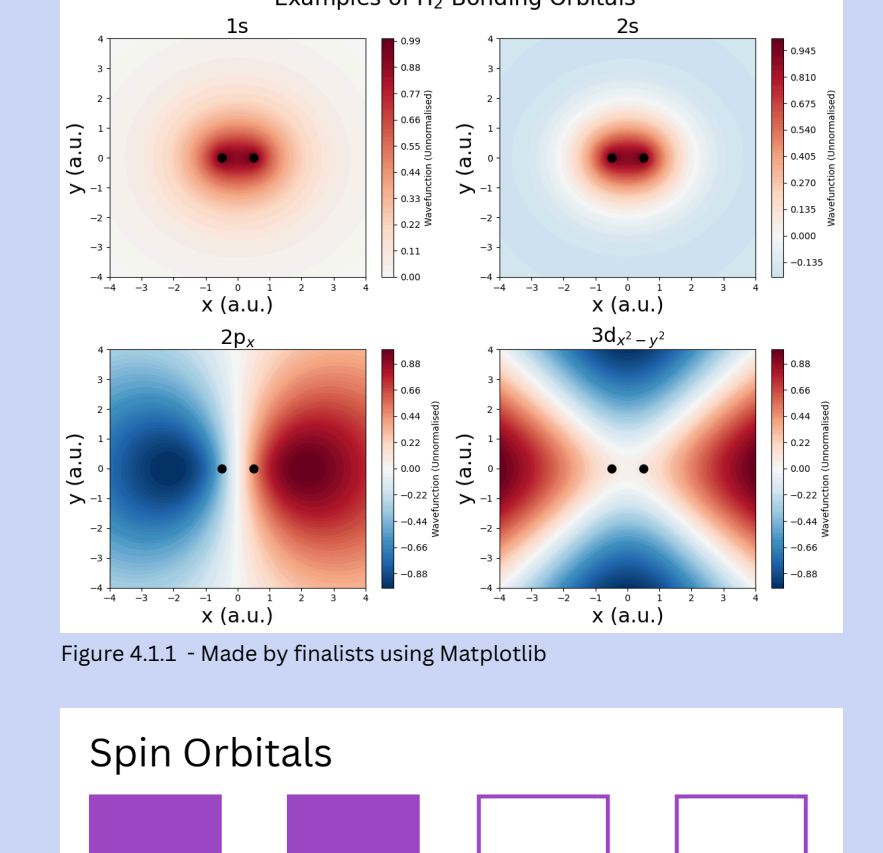
 $|1\rangle_0 \to 1\alpha$ (occupied spin-orbital for α)

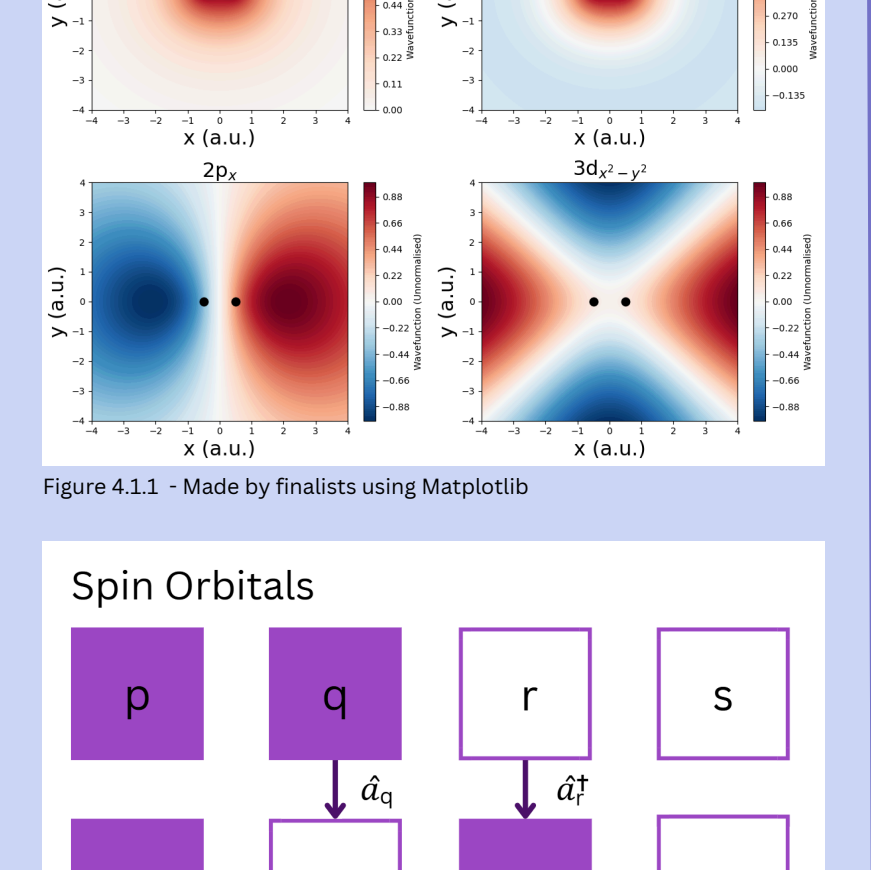
UCCSD Excitations:

 $\theta_{\alpha\beta}: 1\alpha 1\beta \rightarrow 2\alpha 2\beta$

 $\theta_{\alpha}: 1\alpha \to 2\alpha$

 $\theta_{\beta}: 1\beta \rightarrow 2\beta$





2. Fermionic Mappings

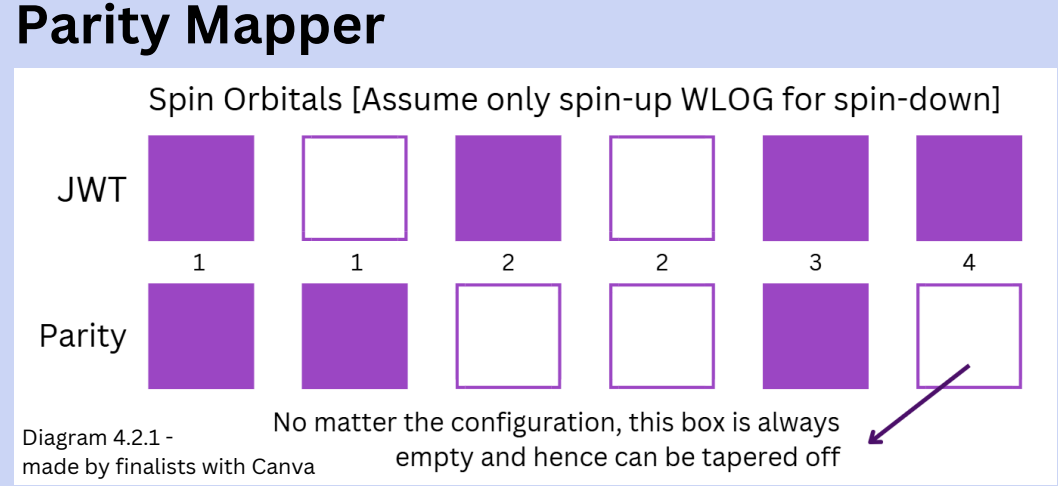
The Jordan-Wigner Transformation [JWT]:

- converts a fermionic Hamiltonian to a qubit Hamiltonian
- maps creation and annihilaton operators to **Pauli operators**

 $\tilde{a}_p|z_0\ldots,z_{p-1},1,z_{p+1},\ldots,z_{N-1}\rangle = (-1)^{\sum_{q=0}^{p-1}z_q}|z_0\ldots,z_{p-1},0,z_{p+1},\ldots,z_{N-1}\rangle$ $\tilde{a}_p|z_0\dots,z_{p-1},0,z_{p+1},\dots,z_{N-1}\rangle = 0$ (5) $\tilde{a}_{p}^{\dagger}|z_{0},\ldots,z_{p-1},0,z_{p+1},\ldots,z_{N-1}\rangle = (-1)^{\sum_{q=0}^{p-1}z_{q}}|z_{0},\ldots,z_{p-1},1,z_{p+1},\ldots,z_{N-1}\rangle$

 $\tilde{a}_{p}^{\dagger}|z_{0},\dots,z_{p-1},1,z_{p+1},\dots,z_{N-1}\rangle=0$ (6)

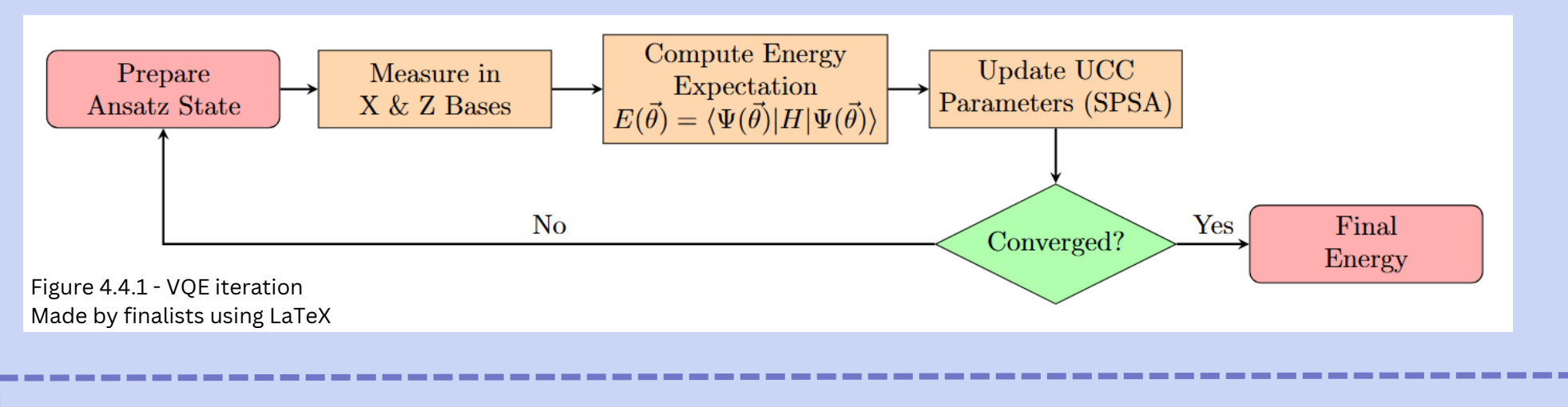
Expressing the above in $a_j^{\dagger} = \frac{1}{2}(X_j - iY_j) \prod_{j=1}^{j-1} Z_k \quad a_j = \frac{1}{2}(X_j + iY_j) \prod_{j=1}^{j-1} Z_k \quad (7)$ terms of Pauli Matrices:

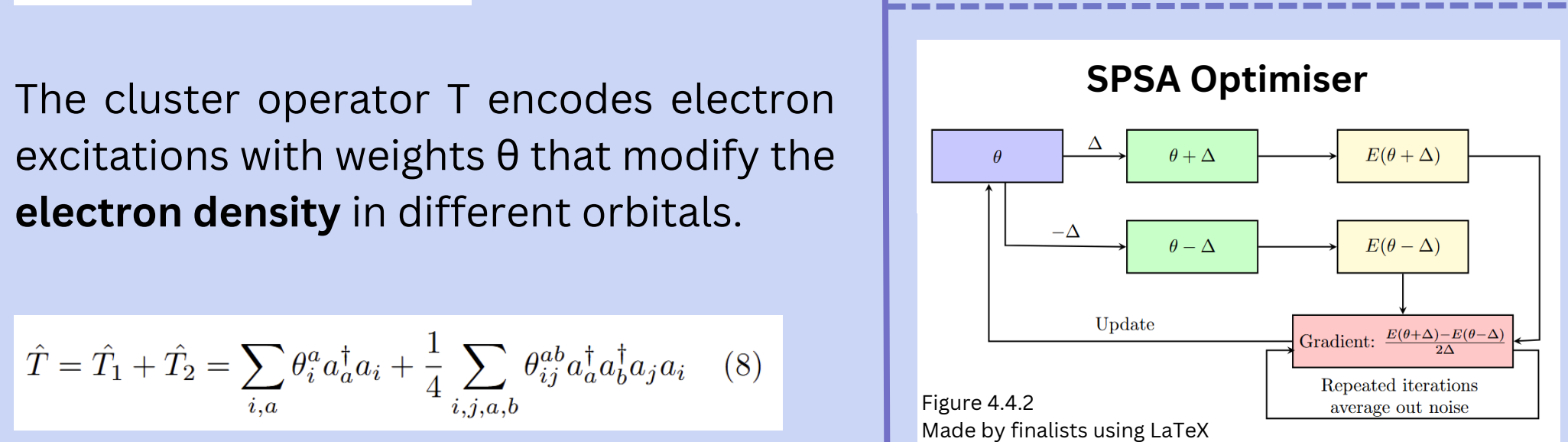


Some states are impossible and qubits can be tapered off to improve efficiency.

- Spin must be conserved
- Total number of electrons is constant

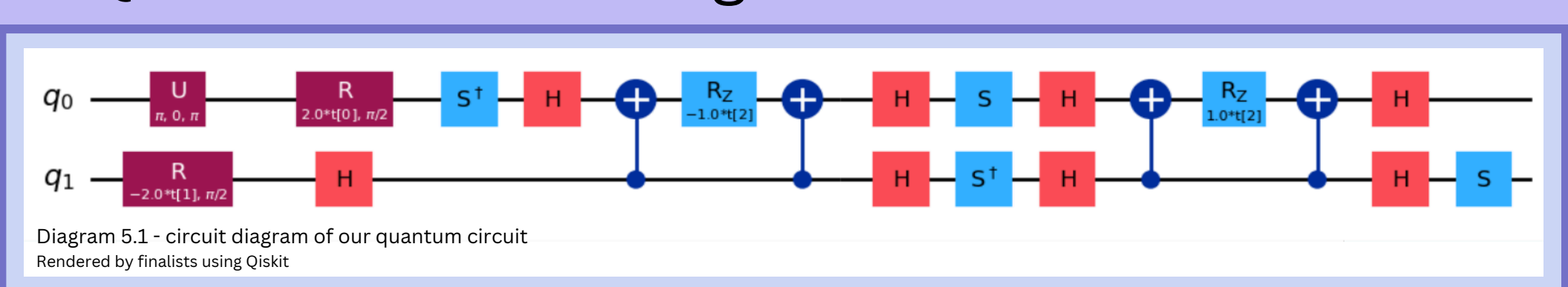
4. Measurement and Optimisation





Perturbation Simultaneous Stochastic Approximation (SPSA) algorithm is typically used due to its effectiveness in noisy environments. Noisy effects tend to cancel out across multiple iterations due to its stochastic nature.

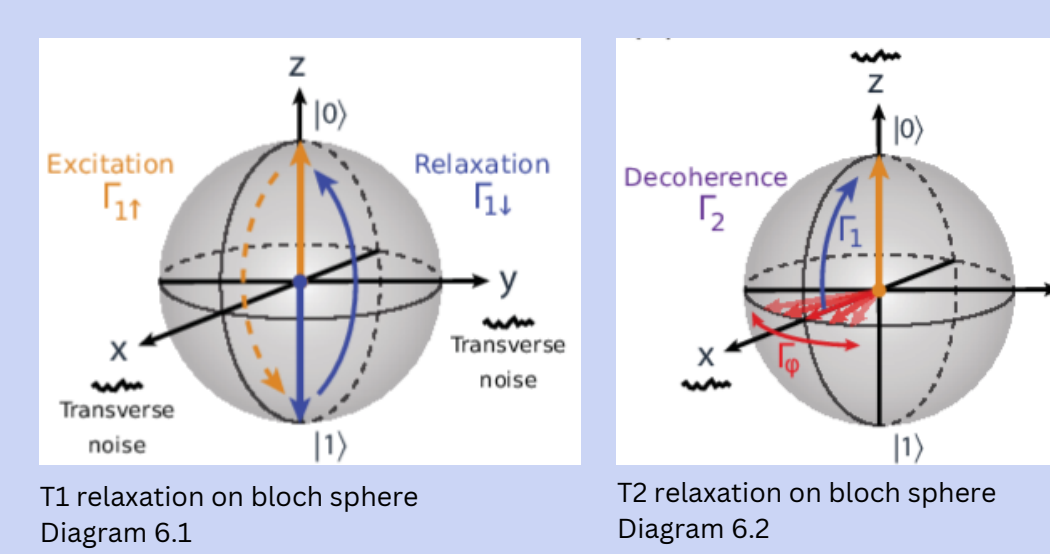
5 - Quantum Circuit Diagram

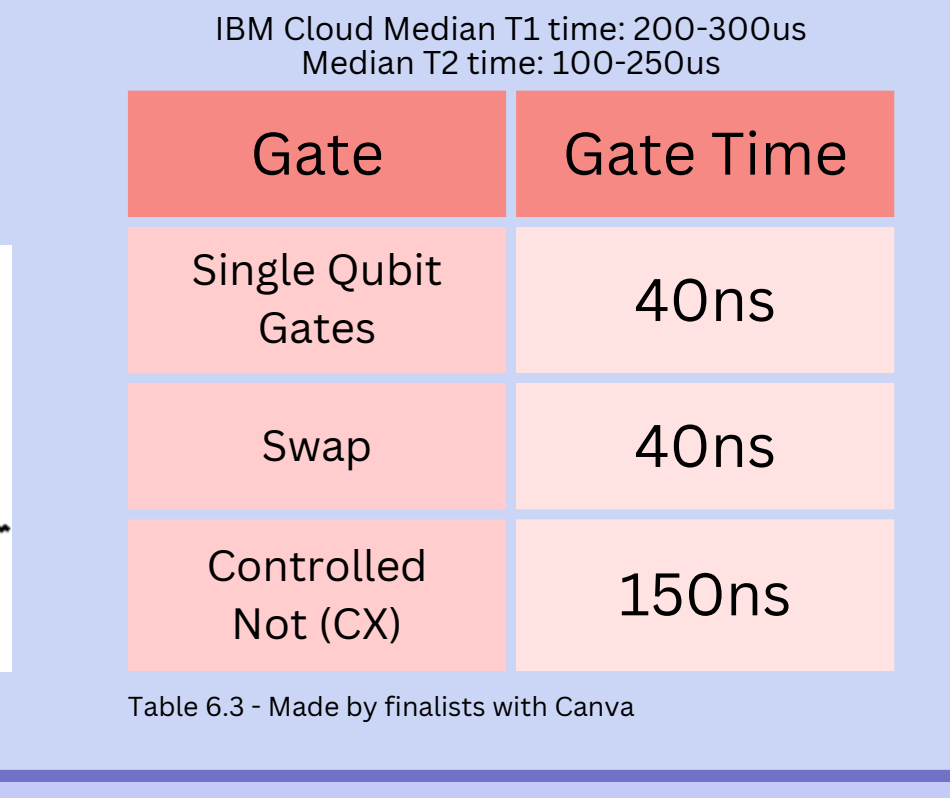


6 - Thermal Relaxation Noise

Qubits face noise from many sources. Besides measurement and readout noise, 2 critical parameters in characterising such noise are T1 and T2 times.

- T1: **lifetime** of a qubit's excited state [\propto time to relax from |1 \rangle to |0 \rangle]
- T2: **coherence** of superposition
- [\propto time to lose its relative phases]





Superconducting

Qubits Noise Levels

7 - Implementation and Graph Plotting

By varying the H-H distance, we used VQE in a noiseless simulation to map the energy landscape [Fig. 8.1]. To find the true ground state energy and optimal geometry, we concurrently optimized interatomic distance and electron excitation parameters using a custom algorithm [Fig. 8.2, noisy conditions].

We then explored noise effects—specifically **thermal relaxation**—with T₁ set to 2T₂. Averaging 20 runs per point yielded a smooth curve described by the product of an **exponential decay and inverse power function** [Fig. 8.3].

For all graphs, we compare our results with Self Consistent Field [SCF] and Full Configuration Interaction [FCI], where FCI offers the most accurate energy. Closer agreement with FCI indicates a better result.

8 - Results

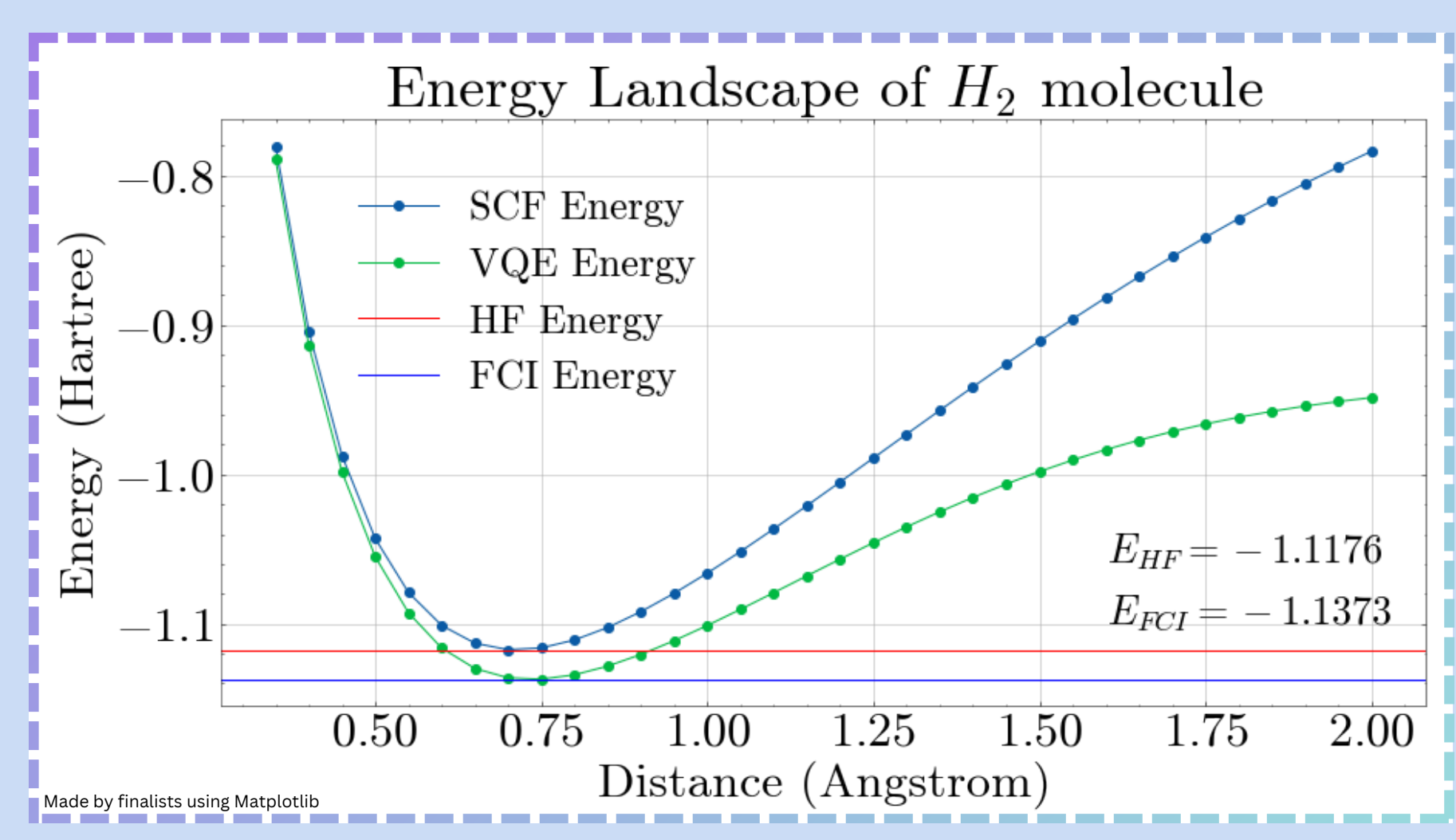


Figure 8.1 - Applying the VQE approach to varying interatomic distances of H₂, the two horizontal lines representing the minimum ground state energy calculated via the 2 different methods [HF and FCI]

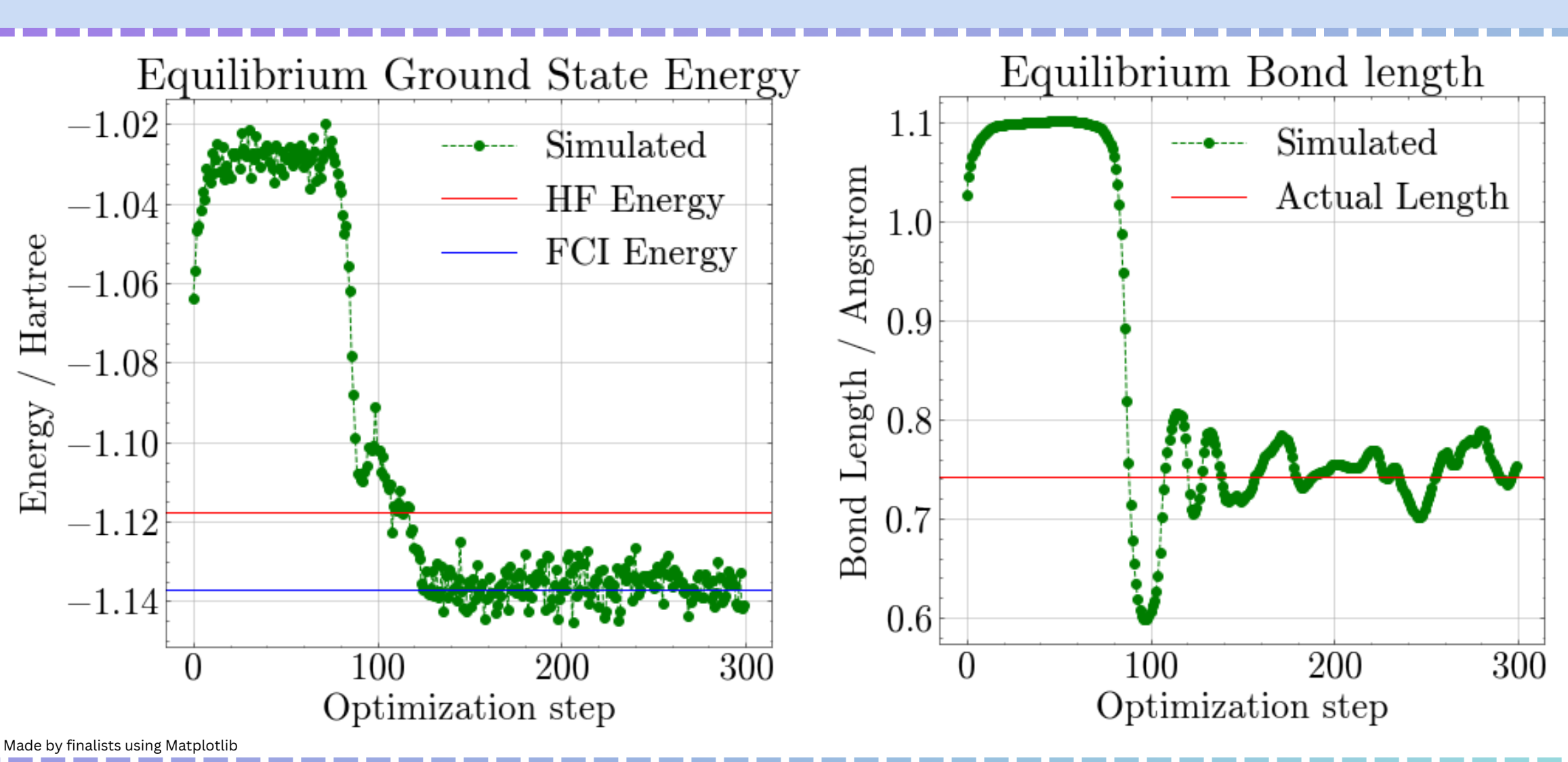


Figure 8.2 - The intermediate results of one execution from our algorithm that optimises interatomic distance [bon length] and electron excitation parameters concurrently.

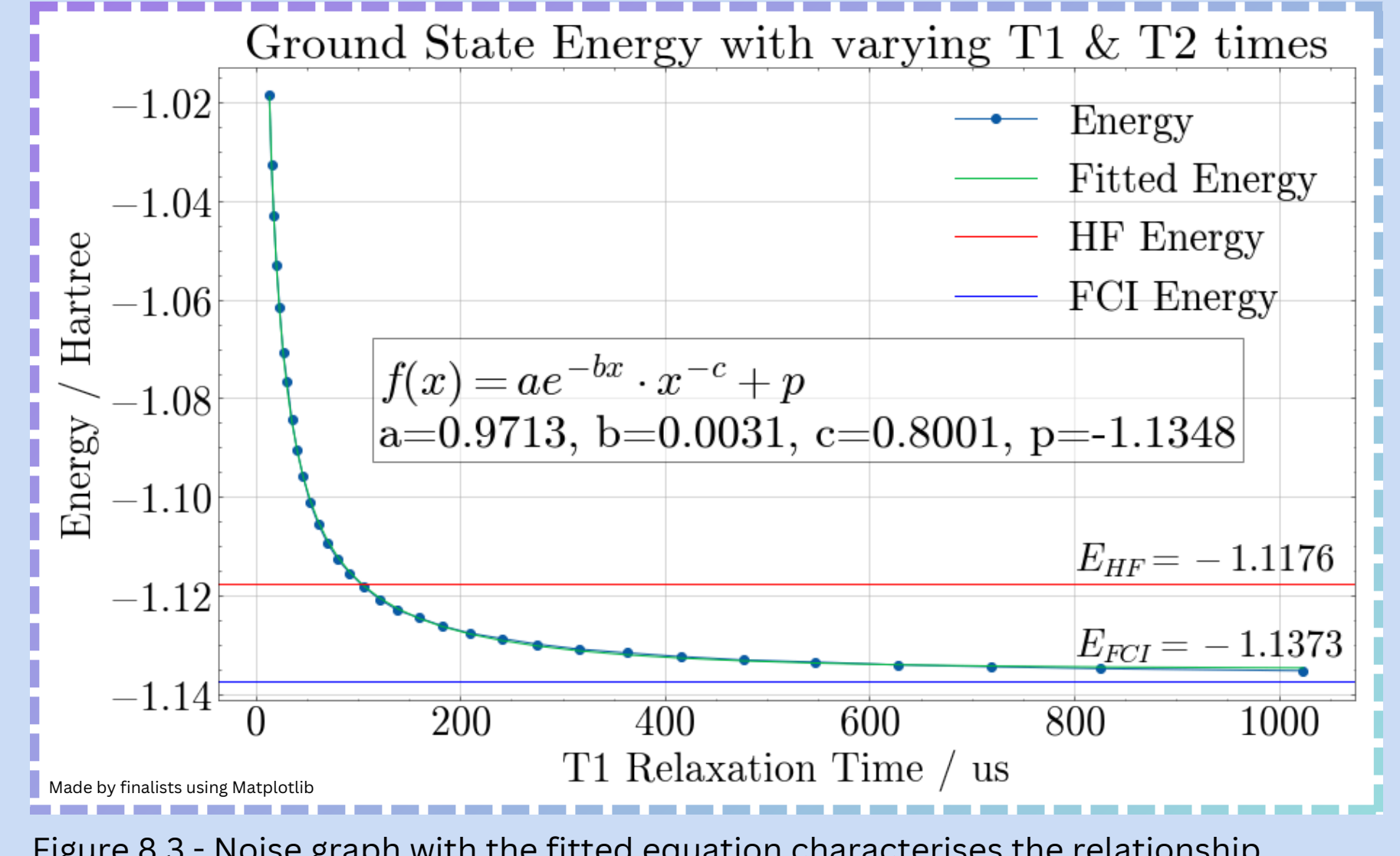


Figure 8.3 - Noise graph with the fitted equation characterises the relationship between thermal relaxation noise and simulation outcome. Energy approaches the FCI Energy as the simulation decreases in noise.

9 - Conclusion

- 1. **VQE is accurate and effective, even under noisy environments.** Extremely close agreement (0.0134% error) of the true ground state energy to FCI energy given by the energy landscape simulation. Concurrent optimisation of molecular geometry and excitation parameters is feasible and yielded great results with **0.11%** error on energy and **1.9%** error on bond length.
- 2. Quantitatively characterised the correlation between thermal relaxation and simulation outcome, modelled as the product of an exponential decay and inverse power function.
- 3. In conclusion, the project is **successful** in meeting its objectives. A comprehensive Jupyter Notebook with code and detailed documentation of the VQE process in quantum chemistry is available on GitHub for future researchers.

10 - Future Work

Investigation into its actual applicability on Quantum Computers

- Requires comparison with the data obtained from running the circuit on an actual Quantum Computer
- If applicable, investigate other parameteres that affect the final graph shape/coefficients
- If not applicable, investigate possible reasons for this discrepancy and if it reflects improvement that could be made to current simulation methods
- Research on Quantum Error Correction Codes (QECC) and their effectiveness in quantum chemistry

Investigation the effectiveness of VQE in simulating more complex molecules

- Likely only achievable on Quantum Computers
- Assess its accuracy, computational resources, and simulation results

References

- [1] Figure 1.5 Taken from Wikipedia before making secondary cropping [https://en.wikipedia.org/wiki/Quantum_logic_gate#/media/File:Quantum_Logic_Gates.png]
- [2] Graphic 1.6 Taken from research paper [https://doi.org/10.1016/j.xcrp.2024.102105] accessed via ScienceDirect [https://www.sciencedirect.com/science/article/pii/S2666386424003837]
- Jared D. Weidman, Manas Sajjan, Camille Mikolas, Zachary J. Stewart, Johannes Pollanen, Sabre Kais, Angela K. Wilson, Quantum computing and chemistry, Published in: Cell Reports Physical Science, Volume 5, Issue 9, 2024, 102105, ISSN 2666-3864, https://doi.org/10.1016/j.xcrp.2024.102105. [3] Diagram 6.1 - Taken from research paper [https://doi.org/10.1063/1.5089550] accessed via ArXiv [https://arxiv.org/abs/1904.06560] Figure 4b
- P. Krantz (MIT, LNS and Goteborg, ITP), M. Kjaergaard (MIT, LNS), F. Yan (MIT, LNS), F. Yan (MIT, LNS), F. Yan (MIT, LNS), S. Gustavsson (MIT, LNS) et al. A quantum engineer's guide to superconducting qubits, Published in: Appl. Phys. Rev. 6 (2019) 2, DOI: 10.1063/1.5089550 [4] Diagram 6.2 - Taken from research paper [https://doi.org/10.1063/1.5089550] accessed via ArXiv [https://arxiv.org/abs/1904.06560] Figure 4d
- P. Krantz (MIT, LNS and Goteborg, ITP), M. Kjaergaard (MIT, LNS), F. Yan (MIT, LNS), T.P. Orlando (MIT, LNS), s. Gustavsson (MIT, LNS) et al. A quantum engineer's guide to superconducting qubits, Published in: Appl.Phys.Rev. 6 (2019) 2, DOI: 10.1063/1.5089550 [5] D. A. Fedorov, B. Peng, N. Govind, and Y. Alexeev. Vge method: A short survey and recent developments, 2021
- [6] Q. Guo and P.-X. Chen. Optimization of vge-ucc algorithm based on spin state symmetry. Frontiers in Physics, 9, 2021.
- [7] M. Qing and W. Xie. Use vqe to calculate the ground energy of hydrogen molecules on ibm quantum, 2023
- [8] J. Tilly, H. Chen, S. Cao, D. Picozzi, K. Setia, Y. Li, E. Grant, L. Wossnig, I. Rungger, G. H. Booth, and J. Tennyson. The variational quantum eigensolver: A review of methods and best practices. Physics Reports, 986:1–128, Nov. 2022. [9] A. Anand, P. Schleich, S. Alperin-Lea, P. W. K. Jensen, S. Sim, M. D'iaz-Tinoco, J. S. Kottmann, M. Degroote, A. F. Izmaylov, and A. Aspuru-Guzik. A quantum computing view on unitary coupled cluster theory. Chemical Society Reviews, 51(5):1659–1684, 2022.